

1 **Dopamine neurons change their tuning according to courtship context in singing birds**

2 Vikram Gadagkar<sup>1</sup>, Pavel A. Puzerey<sup>1</sup>, and Jesse H. Goldberg<sup>1\*</sup>

3 <sup>1</sup>Department of Neurobiology and Behavior, Cornell University, Ithaca, NY 14853, U.S.A.

4 \*Corresponding author. E-mail: [jessegoldberg@gmail.com](mailto:jessegoldberg@gmail.com)

5

6 **Attending to mistakes while practicing alone provides opportunities for learning<sup>1,2</sup>,**  
7 **but self-evaluation during audience-directed performance could distract from ongoing**  
8 **execution<sup>3</sup>. It remains unknown how animals switch between practice and performance**  
9 **modes, and how evaluation systems process errors across distinct performance contexts.**  
10 **We recorded from striatal-projecting dopamine (DA) neurons as male songbirds**  
11 **transitioned from singing alone to singing female-directed courtship song. In the presence**  
12 **of the female, singing-related performance error signals were reduced or gated off and DA**  
13 **neurons were instead phasically activated by female vocalizations. Mesostriatal DA**  
14 **neurons can thus dynamically change their tuning with changes in social context.**

15 When a male zebra finch sings its courtship song to a female of interest, song is highly  
16 stereotyped and tonic levels of dopamine (DA) are increased in Area X, a vocal motor basal  
17 ganglia nucleus capable of regulating song variability<sup>4-8</sup>. Yet when males practice alone, song is  
18 highly variable and tonic DA levels are decreased in Area X<sup>4,9</sup>. Blockade or disruption of striatal  
19 DA signaling eliminates the social context-dependent transition between ‘practice’ and female-  
20 directed ‘performance’ modes<sup>10,11</sup>, suggesting that tonic DA levels actively regulate ongoing  
21 vocal variability<sup>5,7,8,12</sup>.

22 DA has an additional learning function during singing distinct from, and difficult to  
23 reconcile with, its role in modulating vocal variability during courtship<sup>7,13</sup>. Specifically, when

24 males sing alone, Area X projecting DA neurons in the ventral tegmental area (VTax) encode  
25 phasic error signals, necessary and sufficient for learning<sup>14-16</sup>, characterized by brief suppressions  
26 following worse-than-predicted song syllable outcomes and activations following better-than-  
27 predicted ones (Fig. 1a)<sup>17</sup>. Phasic DA signals thus encode errors in predicted song quality, i.e. the  
28 difference between how good a syllable sounded and how good it was predicted to sound based  
29 on recent practice.

30 Do the same songbird DA neurons that modulate ongoing vocal variability also evaluate  
31 recent vocal performance for learning, and if so, how? In mammals, it has been proposed that the  
32 state-dependent vigor of ongoing behavior is regulated by the tonic discharge of DA neurons,  
33 while the evaluation of reward outcomes for learning is regulated by brief, phasic error signals in  
34 the same neurons<sup>18-21</sup>. To test this hypothesis, it is necessary to observe how tonic firing rates and  
35 phasic error signals change (or don't change) in single neurons across clear-cut, DA-dependent  
36 changes in behavioral state. This experiment is uniquely possible in songbirds singing alone or  
37 singing female-directed courtship song (Fig. 1).

38 To test how DA neurons may implement these dual functions, we recorded  
39 antidromically-identified VTax neurons as we controlled both perceived error (with syllable-  
40 targeted distorted auditory feedback (DAF)<sup>17, 22, 23</sup>) and behavioral state (with female present or  
41 absent)<sup>5, 7, 8</sup>. Surprisingly, tonic discharge patterns of VTax neurons, including mean firing rate,  
42 median interspike interval (ISI), burstiness and firing regularity, did not significantly differ  
43 between undirected and directed song (Fig. 2, mean rates: 13.86±3.22 Hz undirected vs.  
44 14.66±3.48 Hz female-directed; median ISI: 0.046±0.018 s undirected vs 0.045±0.016 s female-  
45 directed; coefficient of variation of the ISI distribution (CV<sub>isi</sub>): 0.88±0.18 undirected vs.  
46 0.89±0.19 female-directed; peak of the normalized spike train autocorrelation: 1.15±0.11

47 undirected vs.  $1.13 \pm 0.12$  female-directed,  $n=8$  neurons;  $p > 0.05$  for all measures, paired two-  
48 sided Wilcoxon signed rank tests). Tonic DA discharge patterns during non-singing periods were  
49 also not substantially affected (Extended Data Fig. 1). Thus previously reported increases in  
50 striatal DA levels and associated reduction in courtship song variability<sup>4-7, 12</sup> are unlikely to be  
51 caused by changes in DA spiking activity, suggesting a role for spiking-independent regulation  
52 of DA release or re-uptake at striatal synapses<sup>24-26</sup>.

53 To test how the transition to female-directed song affects phasic error signals, we  
54 recorded neuronal responses to syllable-targeted DAF<sup>17, 22, 23</sup> as males sang alone and to a  
55 female. DAF, though not generally aversive<sup>27</sup>, induces a perceived vocal error on distorted  
56 renditions such that undistorted renditions are reinforced<sup>22, 23</sup> by phasic DA signals<sup>14-16</sup>.  
57 Consistent with past work<sup>17</sup>, VTax neurons recorded during undirected singing exhibited phasic  
58 error signals characterized by suppressions following distortions and phasic activations at the  
59 precise moment of the song when a predicted distortion did not occur (significant error response  
60 in 7/8 VTax neurons, Methods). Significant suppressions followed DAF onset with a latency of  
61  $63 \pm 14$  ms, lasted  $67 \pm 21$  ms, and resulted on average in a  $55 \pm 16\%$  reduction in firing rate  
62 (significant suppressions observed in 6/7 VTAerror neurons, Methods). Significant phasic  
63 activations mirrored phasic suppressions: they followed undistorted target onsets with a latency  
64 of  $46 \pm 25$  ms, lasted  $64 \pm 14$  ms, and resulted on average in a  $37 \pm 10\%$  increase in firing rate  
65 (significant activations observed in 6/7 VTAerror neurons, Methods) (Fig. 3).

66 Phasic error responses that were robust during undirected singing were usually gated off  
67 during courtship song (z-scored error responses, undirected:  $2.6 \pm 0.5$ ; directed:  $1.1 \pm 1.3$ ;  $p < 0.05$ ,  
68 paired two-sided Wilcoxon signed rank test, loss of significant error response in 6/7 VTAerror  
69 neurons, Methods) (Fig. 3).

70           We wondered if reduced performance error signaling during female-directed song could  
71 occur if the male attended less to evaluating his own song and more to real-time interaction with  
72 the female. Although female zebra finches do not sing, they can respond to male courtship  
73 efforts with vocal calls of her own<sup>28</sup>. Consistent with the idea that phasic DA signals can depend  
74 on female behavior, female calls induced phasic activations in every VTAx DA neuron recorded  
75 in sessions where female calls were produced. The timing and magnitude of female call-induced  
76 activations resembled the phasic activations observed following undistorted targets during  
77 undirected singing (latency from call onset:  $39 \pm 24$  ms, duration:  $93 \pm 28$  ms,  $42 \pm 17\%$  increase in  
78 firing rate,  $p < 0.05$  in 7/7 neurons, bootstrap).

79           Together these findings show, for the first time to our knowledge, that tonic DA spiking  
80 is not strongly activated during courtship behavior, that the tuning of DA neurons can  
81 dynamically change with social context, that DA neurons can be phasically activated by vocal  
82 signals of a potential mate, and, more generally, that mistakes are processed differently during  
83 ‘practice’ and audience-directed ‘performance’ modes.

84

85

## 86 References

- 87 1. Sutton, R.S. & Barto, A.G. *Reinforcement learning: an introduction* (MIT Press,  
88 Cambridge, MA, 1998).
- 89 2. Dhawale, A.K., Smith, M.A. & Ölveczky, B.P. The role of variability in motor learning.  
90 *Annual review of neuroscience* **40**, 479-498 (2017).
- 91 3. Ericsson, K.A., Nandagopal, K. & Roring, R.W. Toward a science of exceptional  
92 achievement. *Annals of the New York Academy of Sciences* **1172**, 199-217 (2009).
- 93 4. Ihle, E.C., van der Hart, M., Jongsma, M., Tecott, L.H. & Doupe, A.J. Dopamine  
94 physiology in the basal ganglia of male zebra finches during social stimulation. *Eur J Neurosci*  
95 **41**, 1506-1514 (2015).
- 96 5. Leblois, A. Social modulation of learned behavior by dopamine in the basal ganglia:  
97 Insights from songbirds. *J Physiol Paris* (2012).
- 98 6. Riters, L.V. The role of motivation and reward neural systems in vocal communication in  
99 songbirds. *Front Neuroendocrinol* **33**, 194-209 (2012).
- 100 7. Woolley, S.C. Dopaminergic regulation of vocal-motor plasticity and performance.  
101 *Current opinion in neurobiology* **54**, 127-133 (2019).
- 102 8. Kojima, S., Kao, M.H., Doupe, A.J. & Brainard, M.S. The avian basal ganglia are a  
103 source of rapid behavioral variation that enables vocal motor exploration. *J Neurosci* (2018).
- 104 9. Sasaki, A., Sotnikova, T.D., Gainetdinov, R.R. & Jarvis, E.D. Social context-dependent  
105 singing-regulated dopamine. *J Neurosci* **26**, 9010-9014 (2006).
- 106 10. Leblois, A., Wendel, B.J. & Perkel, D.J. Striatal dopamine modulates basal ganglia  
107 output and regulates social context-dependent behavioral variability through D1 receptors. *J*  
108 *Neurosci* **30**, 5730-5743 (2010).
- 109 11. Murugan, M., Harward, S., Scharff, C. & Mooney, R. Diminished FoxP2 Levels Affect  
110 Dopaminergic Modulation of Corticostriatal Signaling Important to Song Variability. *Neuron* **80**,  
111 1464-1476 (2013).
- 112 12. Hara, E., Kubikova, L., Hessler, N.A. & Jarvis, E.D. Role of the midbrain dopaminergic  
113 system in modulation of vocal brain activation by social context. *Eur J Neurosci* **25**, 3406-3416  
114 (2007).
- 115 13. Fee, M.S. & Goldberg, J.H. A hypothesis for basal ganglia-dependent reinforcement  
116 learning in the songbird. *Neuroscience* **198**, 152-170 (2011).
- 117 14. Hisey, E., Kearney, M.G. & Mooney, R. A common neural circuit mechanism for  
118 internally guided and externally reinforced forms of motor learning. *Nature neuroscience*, 1  
119 (2018).
- 120 15. Xiao, L., *et al.* A Basal Ganglia Circuit Sufficient to Guide Birdsong Learning. *Neuron*  
121 **98**, 208-221 e205 (2018).
- 122 16. Hoffmann, L.A., Saravanan, V., Wood, A.N., He, L. & Sober, S.J. Dopaminergic  
123 Contributions to Vocal Learning. *J Neurosci* **36**, 2176-2189 (2016).
- 124 17. Gadagkar, V., *et al.* Dopamine neurons encode performance error in singing birds.  
125 *Science* **354**, 1278-1282 (2016).
- 126 18. Floresco, S.B., West, A.R., Ash, B., Moore, H. & Grace, A.A. Afferent modulation of  
127 dopamine neuron firing differentially regulates tonic and phasic dopamine transmission. *Nat*  
128 *Neurosci* **6**, 968-973 (2003).
- 129 19. Grace, A. Phasic versus tonic dopamine release and the modulation of dopamine system  
130 responsivity: a hypothesis for the etiology of schizophrenia. *Neuroscience* **41**, 1-24 (1991).

- 131 20. Niv, Y., Daw, N.D., Joel, D. & Dayan, P. Tonic dopamine: opportunity costs and the  
132 control of response vigor. *Psychopharmacology (Berl)* **191**, 507-520 (2007).  
133 21. Schultz, W. Behavioral dopamine signals. *Trends Neurosci* **30**, 203-210 (2007).  
134 22. Tumer, E.C. & Brainard, M.S. Performance variability enables adaptive plasticity of  
135 'crystallized' adult birdsong. *Nature* **450**, 1240-1244 (2007).  
136 23. Andalman, A.S. & Fee, M.S. A basal ganglia-forebrain circuit in the songbird biases  
137 motor output to avoid vocal errors. *Proc Natl Acad Sci U S A* **106**, 12518-12523 (2009).  
138 24. Dreyer, J.K., Herrik, K.F., Berg, R.W. & Hounsgaard, J.D. Influence of phasic and tonic  
139 dopamine release on receptor activation. *J Neurosci* **30**, 14273-14283 (2010).  
140 25. Sulzer, D., Cragg, S.J. & Rice, M.E. Striatal dopamine neurotransmission: regulation of  
141 release and uptake. *Basal ganglia* **6**, 123-148 (2016).  
142 26. Berke, J.D. What does dopamine mean? *Nature neuroscience*, 1 (2018).  
143 27. Murdoch, D., Chen, R. & Goldberg, J.H. Place preference and vocal learning rely on  
144 distinct reinforcers in songbirds. *Sci Rep* **8**, 6766 (2018).  
145 28. Zann, R.A. *The zebra finch: a synthesis of field and laboratory studies*. (Oxford  
146 University Press., 1996).

147

## 148 **Acknowledgments**

149 We thank members of the Goldberg Lab for comments on the manuscript and Samantha  
150 Carouso-Peck and Michael H. Goldstein for help with social context manipulation. VG was  
151 supported by a Simons Foundation Postdoctoral Fellowship and a NIH/NINDS Pathway to  
152 Independence Award (grant # K99NS102520), PAP by NIH/NINDS (grant # F32NS098634),  
153 and JHG by NIH/NINDS (grant # R01NS094667), Pew Charitable Trusts, and Klingenstein  
154 Neuroscience Foundation.

155

## 156 **Author Contributions**

157 VG and JHG designed the research, analyzed data, and wrote the paper. VG and PAP performed  
158 experiments.

159

## 160 **Competing interests**

161 The authors declare no competing financial interest.

162 **Additional information**

163 Data can be accessed at <http://www.nbb.cornell.edu/goldberg/>

164

165

166

167

168

169

170

171

172

173

174

175

176

177

178

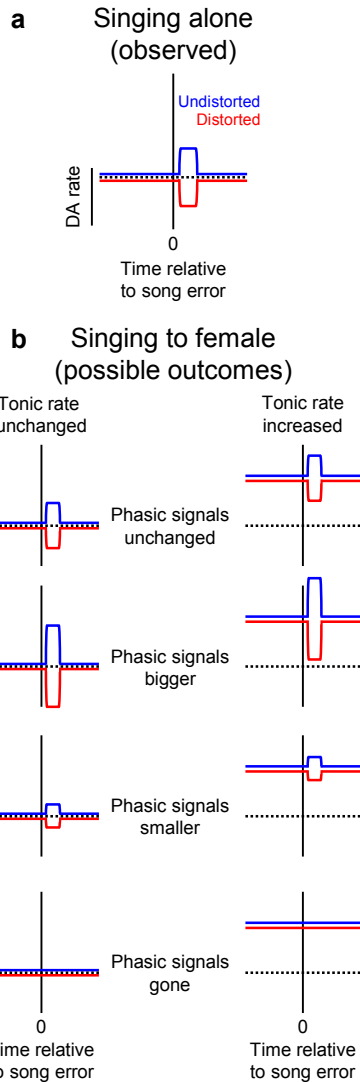
179

180

181

182

183



184

185 **Figure 1. Testing how courtship context affects tonic and phasic dopamine signals. (a)**

186 When singing alone, VTax DA neurons exhibit a low baseline ‘tonic’ firing rate as well as

187 phasic activations and suppressions following undistorted (blue) and distorted (red) syllable

188 renditions, respectively<sup>17</sup> (black dotted line indicates baseline firing rate when singing alone). **(b)**

189 Schematic of possible outcomes for a VTax neuron recorded during female directed song. Tonic

190 rate could either increase (right column) or not (left column). From top to bottom: phasic error

191 signals could be unchanged, bigger, smaller or be gated off altogether. Other possible outcomes

192 (e.g. tonic rate could decrease, phasic activations and suppressions could be independently



193 altered) are not shown. Black dotted lines denote baseline firing rate when male sings alone.

194

195

196

197

198

199

200

201

202

203

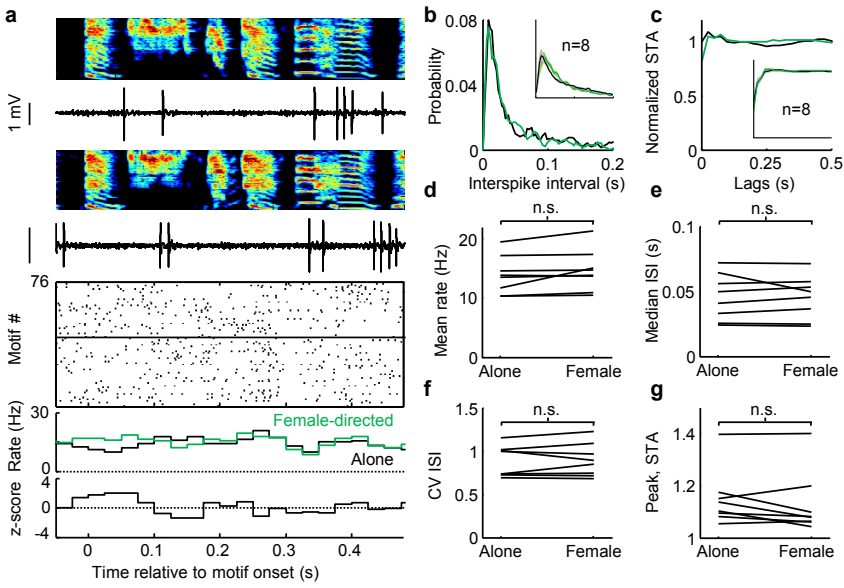
204

205

206

207

208



209

210 **Fig. 2. The tonic discharge of VTax DA neurons during singing does not depend on**

211 **courtship context. (a)** Top to bottom: spectrograms, spiking activity during female-directed and

212 undirected songs, corresponding spike raster plots and rate histograms, and z-scored difference in

213 firing between undirected and directed motif-aligned rate histograms (all plots aligned to motif

214 onset). **(b-c)** ISI distribution (b) and normalized spike train autocorrelogram (STA) (c) during

215 singing alone (black) and female directed (green) songs for the neuron shown in a. Insets: ISI

216 distributions (b) and STAs (c) for 8 VTax neurons (mean +/- SEM shading). **(d-g)** Mean firing

217 rate (d), median ISI (e), coefficient of variation of the ISI distribution (CV<sub>ISI</sub>) (f), and peak of the

218 STA (g) for 8 VTax neurons recorded when males sang alone and when they sang female-

219 directed song (n.s. denotes  $p > 0.05$ , paired two-sided Wilcoxon signed rank test).

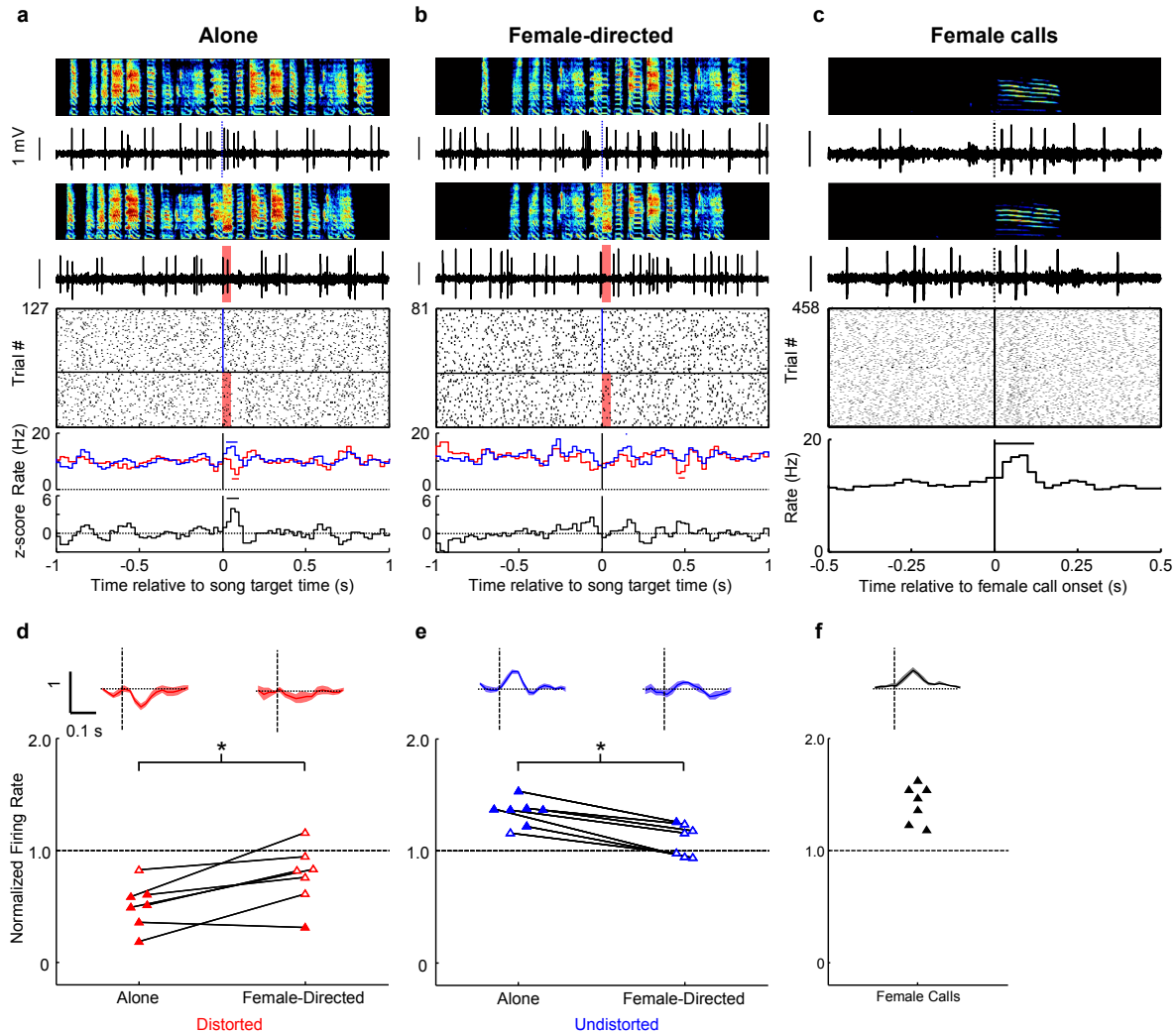
220

221

222

223

224



225

226 **Fig. 3. Phasic DA error signals change their tuning according to courtship context.** Error

227 responses during singing alone (a) and female-directed singing (b) for the same antidromically

228 identified VTax neuron. Top to bottom: spectrograms, spiking activity during undistorted and

229 distorted trials, corresponding spike raster plots and rate histograms, and z-scored difference

230 between undistorted and distorted rate histograms (all plots aligned to target onset). Horizontal

231 bars in histograms indicate significant deviations from baseline ( $p < 0.05$ , one-sided z test). (c)

232 Response to female calls for the same antidromically identified VTax neuron. Top to bottom:

233 spectrograms of female calls and spiking activity, corresponding spike raster plot, and rate

234 histograms (all plots aligned to female call onset). Horizontal bars in histograms indicate

235 significant deviations from baseline ( $p < 0.05$ , one-sided z test). (d) Top, normalized responses to  
236 distorted targets (mean  $\pm$  SEM). Bottom, scatter plot of normalized rate in the 50 to 125 ms  
237 window following target time (solid fills indicate  $p < 0.05$ , bootstrap, Methods) for undirected  
238 and female-directed singing (\* denotes  $p < 0.05$ , paired two-sided Wilcoxon signed rank test). (e)  
239 Same as (d) but for undistorted targets. (f) Top, normalized responses to female calls (mean  $\pm$   
240 SEM). Bottom, scatter plot of normalized rate in the 50 to 125 ms window following female calls  
241 onset (solid fills indicate  $P < 0.05$ , bootstrap, Methods).

242

243

244

245

246

247

248

249

250

251

252

253

254

255

256

257

258

259 **Supplemental Text**

260           During non-singing periods in between female-directed song bouts, male birds exhibit  
261 motivated pursuit-like behaviors, including orienting, and producing vocal calls towards the  
262 female<sup>28</sup>. VTax neurons exhibited a small but significant increase in mean firing rate during  
263 non-singing periods with the female present (mean rates: 11.69±2.88 Hz undirected vs.  
264 12.83±3.05 Hz female-directed,  $p < 0.01$ ; median ISI: 0.068±0.020 s undirected vs 0.061±0.017 s  
265 female-directed,  $p < 0.05$ ), but discharge patterns measured by CVisi and STA did not differ  
266 (CVisi): 0.77±0.21 undirected vs. 0.79±0.19 female-directed,  $p > 0.5$ ; peak of the normalized  
267 STA: 1.11±0.11 undirected vs. 1.09±0.08 female-directed,  $p > 0.5$ , paired two-sided Wilcoxon  
268 signed rank tests) (Extended Data Fig. 1).

269

270

271

272

273

274

275

276

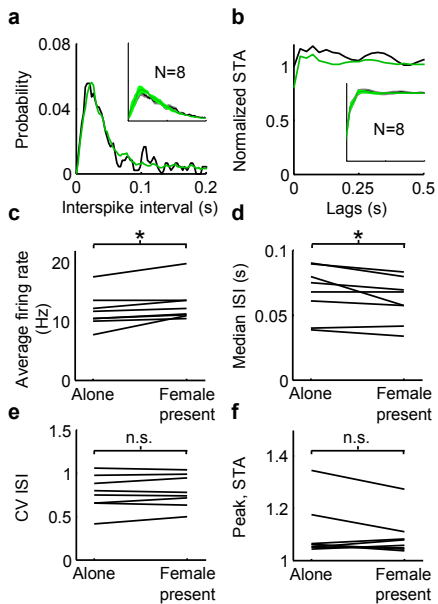
277

278

279

280

281



282

283 **Extended Data Fig. 1 The tonic discharge of VTax DA neurons during non-singing periods**

284 **is subtly affected by courtship context. (a-b)** ISI distribution (a) and normalized spike train

285 auto-correlogram (STA) (b) during non-singing periods with female present (green) and absent

286 (black). Data from the neuron shown in Fig. 2. Insets: ISI distributions (b) and STAs (c) for 8

287 VTax neurons (mean +/- SEM shading). (c-f) Mean firing rate (c), median ISI (d), coefficient of

288 variation of the ISI distribution (CVISI) (e), and peak of the STA (f) for 8 VTax neurons

289 recorded during non-singing periods with female present and absent (\* denotes  $p < 0.05$  and n.s.

290 denotes  $p > 0.05$ , paired two-sided Wilcoxon signed rank test).

291

292

293

294

295

296

## 297 **Methods**

298 **Animals and surgery.** Subjects were 4 adult male (91-240 days old) and 3 adult female (100-  
299 200 days old) zebra finches. All experiments were carried out in accordance with NIH guidelines  
300 and were approved by the Cornell Institutional Animal Care and Use Committee. During implant  
301 surgeries, birds were anesthetized with isoflurane and a bipolar stimulation electrode was  
302 implanted into Area X at established coordinates (+5.6A, +1.5L relative to lambda and 2.65  
303 ventral relative to pial surface; head angle 20 degrees)<sup>17</sup>. Custom microdrives carrying an  
304 accelerometer, linear actuator, and omemade electrode arrays (5 electrodes, 3-5 MOhms,  
305 microprobes.com) were implanted into a region where antidromically identified VTax neurons  
306 were intraoperatively identified. After each experiment, small electrolytic lesions (30  $\mu$ A for 60  
307 s) were made with the recording electrodes for histological verification of electrode position.  
308 Brains were then fixed, cut into 100  $\mu$ m thick sagittal sections and immuno-stained with  
309 antibodies to tyrosine hydroxylase for histological confirmation of reference lesions among  
310 dopamine neurons as described previously<sup>17</sup>.

311

312 **Syllable-targeted distorted auditory feedback.** Postoperative birds were placed in a sound  
313 isolation chamber equipped with a microphone and two speakers which provided distorted  
314 auditory feedback (DAF). To implement targeted DAF, the microphone signal was analyzed  
315 every 2.5 ms using custom Labview software. Specific syllables were targeted by detecting a  
316 unique inter-onset interval (onset time of previous syllable to onset time of target syllable) using  
317 the sound amplitude as previously described<sup>17</sup>. The targeted syllable was programmed to be  
318 distorted with DAF 50% of the time (actual distortion probability: 48 $\pm$ 3%). DAF was a  
319 broadband sound bandpassed at 1.5-8kHz, the same spectral range of zebra finch song. DAF

320 amplitude was measured with a decibel meter (CEM DT-2 85A) and maintained at less than 90  
321 dB.

322  
323 **Electrophysiology.** Neural signals were band-passed filtered (0.25-15 kHz) in homemade analog  
324 circuits and acquired at 40 kHz using custom Matlab software. Single units were identified as  
325 Area X projecting (VTax) by antidromic identification (stimulation intensities 50-400  $\mu$ A, 200  
326  $\mu$ s on the bipolar stimulation electrode in Area X). All neurons identified as VTax were further  
327 validated by antidromic collision testing<sup>17</sup>.

328  
329 **Data analysis.** For each neuron, spiking data were first collected during undirected song when  
330 the male was singing alone in the sound isolation chamber. The male was then presented with  
331 either an adult female in a separate cage (9/11 neurons) or a video of an adult female displayed  
332 on a screen (2/11 neurons) within the sound isolation chamber. Neurons included in singing  
333 analysis (8/11) were recorded for at least 30 motifs of undirected and 30 motifs of female-  
334 directed song. 3/11 VTax neurons recorded exclusively during female calls were included in the  
335 analysis. Neurons included in female call analysis were recorded during at least 60 renditions of  
336 natural, spontaneous female calls. Spike sorting was performed offline using custom Matlab  
337 software. Instantaneous firing rates (IFR) were defined at each time point as the inverse of the  
338 enclosed interspike interval (ISI). Firing rate histograms were constructed with 25 ms bins and  
339 smoothed with a 3-bin moving average. To calculate the mean rate and median ISI during  
340 singing (Fig. 2d-e), the firing rate and median ISI were averaged over all song motifs, with a  
341 time-window extending 50 ms before to motif-onset to 50 ms after motif-offset. The coefficient  
342 of variation (CV) of the ISI and the peak of the spike-train autocorrelation (STA) in Fig. 2f-g



343 were computed over the entire singing bouts. To test for error responses, we compared the  
344 firing activity between randomly interleaved undistorted and distorted song renditions. We  
345 computed the z-scored difference between the target time-aligned distorted and undistorted firing  
346 rate histograms (Fig. 3a-b). The target time was defined as the median DAF onset-time relative  
347 to the distorted syllable onset-time. The error response was defined as the mean z-scored  
348 difference in a 50-125 ms window following target time<sup>17</sup>. Monte Carlo methods were used to  
349 quantify the significance of rate changes following target times of the song and following female  
350 calls (Fig. 3d-f) as previously described<sup>17</sup>. Briefly, the mean number of spikes within a 50-125  
351 ms window after DAF, undistorted target onset, or female call onset was compared to 10,000  
352 surrogate means generated by calculating the mean number of spikes in an identical number of  
353 randomly placed windows during singing (for undistorted and distorted targets), and during non-  
354 singing periods (for female calls). *P* values for the suppression (or activation) were calculated by  
355 analyzing the frequency with which the surrogate means were less than (or greater than) or equal  
356 to the observed mean (Fig. 3d-f). To quantify the magnitude of significant activation and  
357 suppressions (Fig. 3d-f), we calculated the normalized firing rate as follows: the mean number of  
358 spikes in a 50-125 ms window after DAF target time (or female call onset) was normalized by  
359 the mean number of spikes in 10,000 randomly placed identical windows during singing (for  
360 undistorted, distorted, and female call targets)<sup>17</sup>. To calculate the significance bars shown in Fig.  
361 3a-c, spiking activity within  $\pm 1$  second relative to target onset was binned in a moving window  
362 of 30 ms with a step size of 2 ms. Each bin after the target time was tested against all the bins in  
363 the previous 1 second (the prior) using a one-sided z-test<sup>17</sup>. To calculate the latencies and  
364 durations of significant activations (suppressions), a threshold of half the firing rate histogram  
365 maximum (minimum) was applied to the firing rate histogram. The onset-time was defined as the

366 first increasing (decreasing) threshold-crossing after target time, while the offset was defined as  
367 the first decreasing (increasing) threshold-crossing after onset-time.

368

369 **Data availability.** The data that support the findings of this study are available from the  
370 corresponding author upon reasonable request.

371

372 **Code availability.** The custom Matlab code used in this study are available from the  
373 corresponding author upon reasonable request.

374

375